13th IEA Heat Pump Conference
April 26-29, 2021 Jeju, Korea

Refrigerant Circuitry Optimization of Heat Exchangers for Charge Reduction and Robust Performance in Reversible Heat Pump Application

Zhenning LI[a], Vikrant Aute[a,*], Jiazhen LING[a]

[a]Center for Environmental Energy Engineering
Department of Mechanical Engineering, University of Maryland
College Park, MD 20742 USA

Abstract

Heat pumps are becoming more and more desirable around the world as an efficient mean of space conditioning for both cooling and heating requirements. Heat exchangers (HXs) are the key components in these devices and pose some unique design challenges because the same HX has to operate as an evaporator in one mode and as a condenser in the other. Studies have proved that by optimizing the refrigerant circuitry, the performance of HXs can be significantly improved. In a reversible heat pump application, the optimal circuitry obtained under the air conditioning (AC) mode cannot guarantee optimal performance if it is used in the heat pump (HP) mode. Our study shows that the single objective optimal design obtained under AC mode yields 11.4% capacity degradation when it is used in HP mode. This paper presents a multi-objective refrigerant circuitry optimization approach to achieve robust heat exchanger performance in both cooling and heating modes. This work builds on a newly developed Integer Permutation based Genetic Algorithm (IPGA), which can guarantee good manufacturability of optimal circuitry designs. The enhanced IPGA extends the capabilities to generate designs with splitting and merging circuits, thus exploring the design space thoroughly. Two multi-objective problem formulation is proposed. One formulation aims at minimizing refrigerant charge, and the other formulation aims at maximizing HX capacity. The optimal HX designs are analyzed at the system level as a part of a reversible heat pump simulation. A case study using an A-type indoor unit shows that the optimal design obtained using the formulation to minimize charge can yield charge reduction by 19.2% under AC mode and 21.6% under HP mode. The optimal design using the formulation to maximize capacity improves the cooling capacity by 2.3% and system COP by 2.5% under AC mode and meanwhile, improves the heating capacity by 3.0% and system COP by 2.8% under HP mode. Considering the performance degradation of the single objective optimal, the effective capacity improvement of the bi-objective optimal is 14.4%.

Selection and/or peer-review under responsibility of the organizers of the 13th IEA Heat Pump Conference 2020.

Keywords: Heat exchanger; Circuitry optimization; Genetic Algorithm, Charge reduction, Reversible heat pump

1. Introduction

Tube-fin heat exchangers (TFHXs) are prominent components in air conditioning and heat pump systems. This type of heat exchanger consists of a bundle of tubes with fin sheets. The performance of TFHXs is greatly affected by a large number of structural parameters (tube diameter, tube length, fin type, fin thickness, etc.) and therefore, conducting optimization on such parameters can significantly improve its performance [1]. In addition to those parameters, the configuration of tube connections, i.e. refrigerant circuitry, determines the refrigerant flow path, and also significantly impacts the heat exchanger performance [2-8]. For an existing

* Corresponding author. Tel.: +1-301-405-8726
E-mail address: vikrant@umd.edu

TFHX design with a given geometry, performing optimization on refrigerant circuitry is more convenient and cost effective than varying other structural parameters. For example, changing the circuitry is a matter of changing U-bend length and locations, whereas changing tube-spacing can require new fin dies, which is costly and has much longer lead time.

Researchers have tried to use different tube-fin HX circuitry optimization approaches to obtain the best circuitry under a specific operating condition. Domanski et al. [2] developed an optimization tool called ISHED (Intelligent System of Heat Exchanger Design). This optimization scheme switches between Evolutionary learning and Symbolic learning. They performed comprehensive studies to optimize circuitry of TFHXs as evaporators or condensers [9-11]. Their maximum reported HX capacity improvement from optimization runs and experimental validations are 13% from CO_2 gas cooler [12] and 2.2% from a R410A evaporator [13], respectively. Wu et al. [14; 15] developed another optimization approach, which switches between knowledge-based GA and Simulated Annealing. Moreover, the group created effective operators (greedy crossover and greedy mutation) to improve the convergence. They performed circuitry optimization on 3 evaporators and 1 condenser, and the maximum predicted capacity improvement in their study is 7.4%. Ploskas et al. [16] represented circuitry using an adjacency matrix and constrained the hairpins to be on one side of the HX. By comparing five different derivative-free optimization algorithms, they concluded that TOMLAB/glcDirect and TOMLAB/glcSolve can efficiently find optimal or near-optimal circuitries. In their study, the TFHXs are also optimized under specific operating conditions either as an evaporator or as a condenser.

For a reversible heat pump system, the same TFHX operates as a condenser in one mode and as an evaporator in the other mode. In literature [17], various performance metrics have been used as objectives for the TFHX circuitry optimization studies, however, all reported circuitry optimization are performed under specific refrigerant operating condition. Taking an indoor unit as an example, the optimal circuitry obtained by optimizing the HX as an evaporator in air conditioning mode does not necessarily guarantee desirable performance when the refrigerant flow is reversed, and it operates as a condenser under heat pump mode. It is thus clear that circuitry optimization for HX in reversible heat pump application has not been explored. This paper aims at tackling this challenge.

The remainder of the paper is organized as follows. Section 2 details an enhanced heat exchanger circuitry optimization algorithm. Section 3 presents two multi-objective problem formulations to achieve robust heat exchanger performance in a reversible heat pump. Section 4 presents a case study to demonstrates the efficacy of the proposed circuitry optimization algorithm and compare the bi-objective problem formulations with a single objective problem formulation. Section 5 analyses the optimization results and presents system level simulation results. Section 6 presents the conclusions of this study.

2. Enhanced Integer Permutation based Genetic Algorithm

2.1. Chromosome representation

To conduct optimization using Genetic Algorithm, the first step is to find a mathematical representation of the circuitry. A good individual representation (chromosome) can not only reduce the searching space, but can also simulate the nature of the problem [18]. In our previous research, an Integer Permutation based Genetic Algorithm (IPGA) [17] was developed to obtain the optimal circuitry designs. IPGA represents tubes as a sequence of integers (i.e. integer permutation). For an integer permutation, each integer (i.e., tube number) appears exactly once, thus, any chromosome generated by the Genetic Algorithm can be mapped to a valid circuitry and the size of the search space is dramatically reduced by the elimination of redundant designs. Li and Aute [19] have shown that IPGA demonstrates superior capability to obtain better refrigerant circuitries with lower computational cost than the other methods in literature. Readers are referred to the original paper [19] for more details of the IPGA developed in our previous research.

However, the previous IPGA cannot generate designs with splitting and merging of circuits. In order to remedy this limitation, a new chromosome representation called ‘Split Branch Chromosome’ (Fig. 1(a)) is developed and implemented in the enhanced IPGA. The new chromosome representation uses the concept of jagged arrays, with each element of this array representing a branch of tubes. Each branch contains 3 parts. The 1st part of the branch represents the tube sequence. The 2nd part of the branch represents the upstream tube. The 3rd part of the branch represents the downstream tube. Dummy tube number ‘0’ is used as the place holder in the 2nd part, if the 1st tube of the branch is an inlet tube of a circuit. And dummy tube number ‘-1’ is used as the place holder in the 3rd part, if the last tube of the branch is an outlet tube of a circuit.

Fig. 1(b) shows the chromosome representation of the 24-tube heat exchanger in Fig. 1(a). This sample heat exchanger has one splitting tube (tube # 3) and one merging tube (tube #20). With the ‘Split Branch

Chromosome', number of circuits is flexible, i.e., the optimal number of circuits is also an output from optimization and it can represent circuitry designs with splitting and merging circuits.

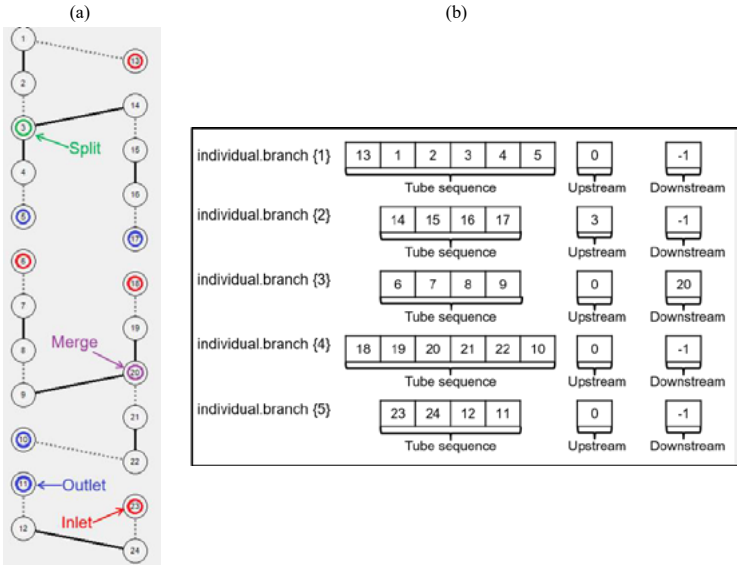

Fig. 1. Chromosome Representation: (a) 24-tube heat exchanger sample; (b) Split branch chromosome

2.2. GA Operators

In Genetic Algorithm, the creation of new individuals relies on the genetic operators. By transforming the selected individual to a new individual with potentially better fitness, the genetic operators direct the search and drive the optimization process.

To adapt the new chromosome representation and extend IPGA's capability to generate designs with splitting and merging circuits, the enhanced IPGA requires new genetic operators. Therefore, two novel genetic operators (Fig. 2) are developed. In order to generate circuit splitting, the split operator in Fig. 2 (a) randomly determine one tube as the splitting tube and make a sub-section of tubes to form a new branch, thus creates a split. Oppositely, the merge operator in Fig. 2 (b) randomly determines one tube as the merging tube and makes a sub-section of tubes to form a new branch, thus creates a merging of circuits.

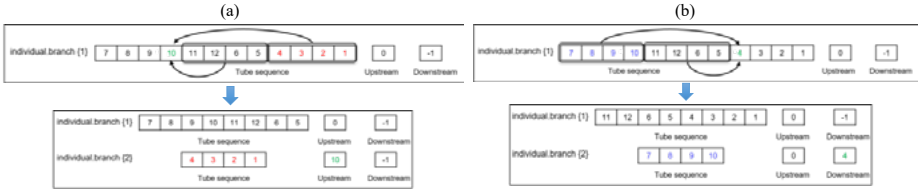

Fig. 2. (a) Split operator; (b) Merge operator

In order to adapt to the change of the chromosome representation, the six GA operators from previous IPGA [17] are modified to form six new GA operators (Fig. 3). The 'gene sequence inversion' operator in Fig. 3(a) chooses a random subsection of a branch and inverts the order of the tubes. The 'gene insertion' operator in Fig. 3(b) puts a randomly selected tube into a random position. The 'in-branch transposition' operator in Fig. 3(c) reverses two randomly chosen tubes inside a single branch, while the 'cross-branch transposition' operator in Fig. 3(d) reverses two randomly selected tubes between different branches. The 'branch detachment' operator in Fig. 3(e) splits a randomly selected branch into two branches. The 'branch union' operator in Fig. 3(f) chooses two branches and unites them into one branch. With the 'branch union' and 'branch detachment' operators, the number of circuits can be varied and optimized in a generic fashion.

Fig. 3. GA Operators: (a) Gene sequence inversion; (b) Gene insertion; (c) In-branch transposition; (d) Cross-branch transposition; (e) Branch detachment; (f) Branch union

3. Problem Formulations

To achieve stable heat exchanger performance in reversible heat pump, two problem formulations are explored. The 1st formulation in Equation (1) aims at maximizing the heat exchanger capacity under different operating conditions. One of the objectives is to maximize the HX capacity when it is operated as an evaporator under cooling mode, and the other objective is to maximize the capacity when it is operated as a condenser under heating mode. The 2nd formulation in Equation (2) aims at minimizing refrigerant charge. One objective is to minimize charge under cooling mode and the other objective is to minimize charge under heating mode. It should be noted that real heat pump systems may use a charge reservoir (e.g., accumulator or receiver) to store charge, but such reservoir is not considered here as the focus is to minimize the charge in the heat exchangers only.

Both problem formulations implement 8 constraints. The first 5 operating constraints limit capacity, refrigerant pressure drop, refrigerant charge, outlet refrigerant saturation ΔT and sensible heat ratio in acceptable ranges as compared with the baseline. The remaining 3 constraints are manufacturability constraints. Specifically, the 6th constraint ensures the inlet and the outlet tubes on the same side of HX. The 7th constraint avoids long U-bends spanning over 2 tube rows. The last constraint avoids partially overlapped U-bends crossing. The manufacturability constraints and the constraint handling scheme are detailed in Li et al. [17].

It is worthwhile to mention that in order to evaluate the performance of the HX under both operating modes, the HX performance under AC mode is first evaluated, then the refrigerant flow direction is reversed (i.e. the inlets and outlets tubes are swapped), and the HX performance under HP mode is evaluated. In addition to the reversion of refrigerant flow direction, the air and refrigerant inlet conditions and the empirical correlations to predict in-tube heat transfer coefficient and pressure drop are also changed to accommodate the switch between AC mode and HP mode.

$$
\begin{aligned}
&\textit{Objective}-1:\ \textit{Maximize}(\mathrm{Q}_{\mathrm{AC\ mode}})\\
&\textit{Objective}-2:\ \textit{Maximize}(\mathrm{Q}_{\mathrm{HP\ mode}})\\
&\textit{Subject to}:\\
&\quad \mathrm{Q} \geq \mathrm{Q}_{\mathrm{baseline}}\\
&\quad \Delta\mathrm{P}_{\mathrm{refrigerant}} \leq \Delta\mathrm{P}_{\mathrm{refrigerant,baseline}}\\
&\quad \mathrm{Charge} \leq \mathrm{Charge}_{\mathrm{baseline}}\\
&\quad \left|\Delta T_{\mathrm{sat}} - \Delta T_{\mathrm{sat,baseline}}\right| \leq 1K\\
&\quad \left|SHR - SHR_{\mathrm{baseline}}\right| \leq 3\%\\
&\quad \text{Inlets and outlets on the same side of HX}\\
&\quad \text{No long U-bend spanning over 2 tube rows}\\
&\quad \text{No overlapped U-bend crossing}
\end{aligned}
\qquad (1)
$$

$$
\begin{aligned}
&\textit{Objective}-1:\ \textit{Minimize}(\text{Refrigerant charge}_{\mathrm{AC\ mode}})\\
&\textit{Objective}-2:\ \textit{Minimize}(\text{Refrigerant charge}_{\mathrm{HP\ mode}})\\
&\textit{Subject to}:\\
&\quad \mathrm{Q} \geq \mathrm{Q}_{\mathrm{baseline}}\\
&\quad \Delta\mathrm{P}_{\mathrm{refrigerant}} \leq \Delta\mathrm{P}_{\mathrm{refrigerant,baseline}}\\
&\quad \mathrm{Charge} \leq \mathrm{Charge}_{\mathrm{baseline}}\\
&\quad \left|\Delta T_{\mathrm{sat}} - \Delta T_{\mathrm{sat,baseline}}\right| \leq 1\ K\\
&\quad \left|SHR - SHR_{\mathrm{baseline}}\right| \leq 3\%\\
&\quad \text{Inlets and outlets on the same side of HX}\\
&\quad \text{No long U-bend spanning over 2 tube rows}\\
&\quad \text{No overlapped U-bend crossing}
\end{aligned}
\qquad (2)
$$

4. Case Studies

An evaporator from an A-type indoor unit (Fig. 4(a)) is used as the baseline for circuitry optimization, because it is experimentally validated in our laboratory. Table 1 shows the structural parameters for the baseline indoor coil. Table 2 shows the operating conditions for the baseline coil working in cooling mode and heating mode. The air side conditions are adopted from ASHRAE Test Standard [20]. The air velocity flow maldistribution at the frontal face of the A-type indoor unit is simulated using an OpenFOAM® based CFD model (Fig. 4(b)), and the air maldistribution profile is imposed on the air side to improve the HX performance prediction. Table 3 lists the empirical correlations used for local heat transfer and pressure drop calculations during the performance evaluation of the HX as an evaporator or a condenser.

Table 1: Structural Parameters and Operating Conditions of Baseline Evaporator

Structural Parameters	Unit	Value
Tube Outer Diameter	mm	9.5
Fins Per Inch	FPI	15
Fin Type	-	Wavy Louver
Tube Length	m	0.503 m
Vertical Spacing	mm	20.0 mm
Horizontal Spacing	mm	25.0 mm
Number of Tube Banks		4
Number of Tubes Per Bank		22

Table 2: Operating Conditions of Baseline Working as an Evaporator and a Condenser

Operating Parameters	Unit	Baseline as Evaporator	Baseline as Condenser
Refrigerant	-	R410A	R410A
Pressure	kPa	1154.55	2432.44
Temperature	◦C	12.03	65.07
Refrigerant Quality	-	0.22	-
Refrigerant Mass Flow Rate	kg/s	0.0312	0.0275
Air Volume Flow Rate	ft^3/min	600	617
Air Pressure	kPa	101.325	101.325
Air Temperature	◦C	26.42	21.23
Air Relative Humidity	%	50.97	58.80

Table 3: Correlations Adopted in HX Simulation

Operating Mode	Heat Transfer Correlations	Pressure Drop Correlations
Refrigerant - Liquid Phase	Dittus and Boelter [21]	Blasius [22]
Refrigerant - Two Phase Boiling (Evaporator)	Jung *et al.* [23]	Jung and Radermacher [24]
Refrigerant - Two Phase Condensation (Condenser)	Cavallini et al. [25]	Lockhart and Martinelli [26]
Refrigerant - Vapor Phase	Dittus and Boelter [21]	Blasius [22]
Air	Wang *et al.* [27]	Wang *et al.* [27]

At the fitness evaluation stage, a finite volume heat exchanger model [28] is used to simulate the performance of the heat exchanger with different circuitries. The model can account for the refrigerant flow maldistribution among different circuits by iterating on the pressure residual at the outlet of each circuit. This

HX model was validated with measured data [29] for the same baseline HX under AC and HP modes, and the deviation between simulations and experiments are below 5% as shown Fig. 4(c).

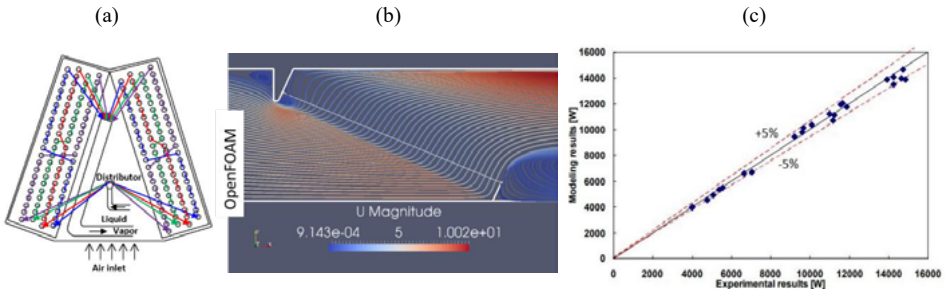

Fig. 4. (a) Baseline Circuitry; (b) Air Maldistribution in A-type Unit Simulated by CFD Model; (c) Experiment Tests vs Simulations

5. Results

5.1. Bi-objective optimization result

In this case study, the GA population size is set to 200, the number of generations is set to 500 and the population replacement ratio is 20% (i.e. the elitism reservation ratio is 80%). Fig. 5(a) shows the Pareto front for Formulation (1) plotted in the objective space. The Pareto front consists of 23 optimal designs. Fig. 5(b) shows the Pareto front using Formulation (2). The X-axis and Y-axis are the refrigerant charge under AC and HP mode. This Pareto front consists 36 optimal designs. Among the optimal designs in two Pareto fronts, the designs whose capacity/charge ranks at the median of the all designs in the Pareto front are sampled for further analysis, since it is expected to exhibit balanced performance under AC and HP modes.

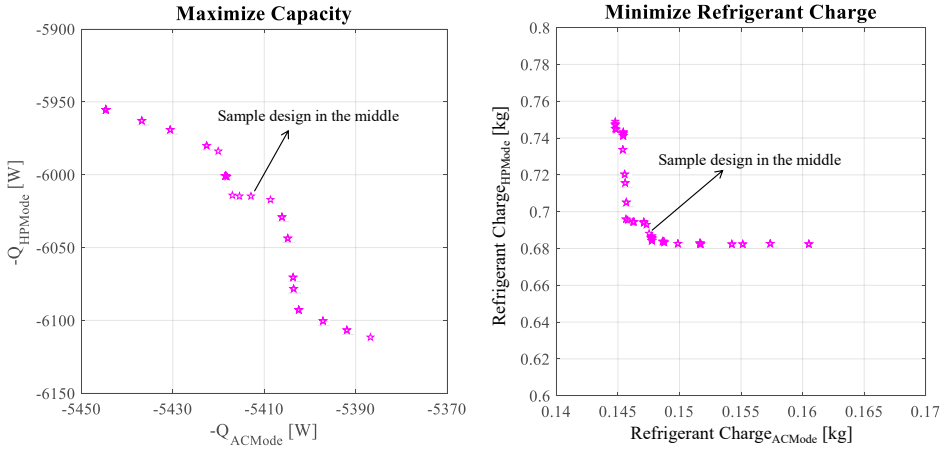

Fig. 5. (a) Pareto Front for Maximizing Capacity; (b) Pareto Front for Minimizing Refrigerant Charge

5.2. Single objective optimization result

To emphasize the necessity to use the multi-objective problem formulation to optimize heat exchangers in reversible heat pumps, the same baseline heat exchanger is optimized solely under air-conditioning mode using a single objective problem formulation. The only objective is to maximize the evaporator cooling capacity under AC mode. The operating constraints and the manufacturability constraints are kept the same as those in Section 3. And the GA settings (the population size, the number of generations and population replacement ratio) are also the same as in the previous practice. Fig. 6(a) shows the GA evolution progress of the single objective optimization. The single objective optimal yields 2.4% capacity improvement under AC mode.

Fig. 6(b) shows the performance comparison between the single objective optimal with the bi-objective optimal to maximize capacity under both AC and HP modes. The bi-objective optimal yields 2.3% capacity increase under AC mode, which is a little less than the improvement of the single objective optimal under AC mode (2.4%). However, if the single objective optimal is used as a condenser in a reversible heat pump, the capacity degrades from 5845 W to 5177 W by 11.4% compared to the baseline. In contrast, the bi-objective optimal still improves condenser capacity by 3.0% under HP mode, it indicates that the effective capacity improvement of bi-objective optimal under HP mode is 14.4% (i.e., 11.4%+3.0%) considering the performance degradation of the single objective optimal under HP mode.

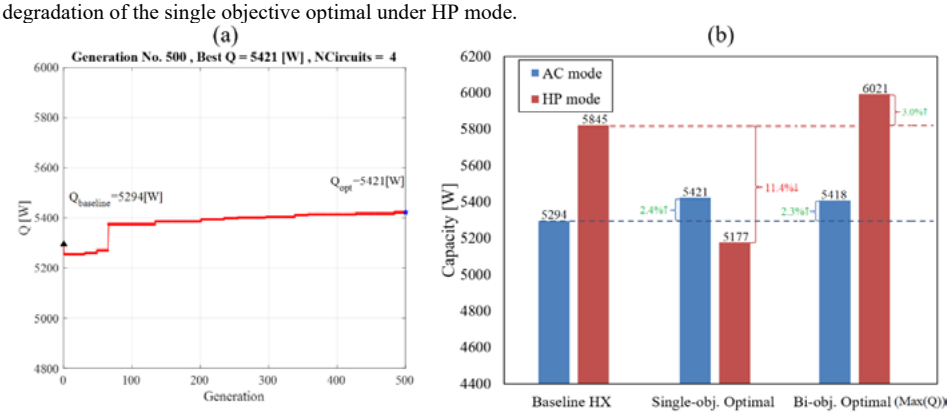

Fig. 6. (a) Single objective optimization GA progress; (b) Comparison of single-obj. with bi-obj. optimal

Table 4 presents the detailed performance of the baseline, the single objective optimal and the bi-objective optimal designs sampled from above Pareto fronts. Compared with the baseline, the optimal design from bi-objective Formulation (1) yields a capacity increase of 2.3% when it is used as an evaporator under AC mode and it yields the capacity increase of 3.0% when it is used as a condenser under HP mode. This indicates that its circuitry design is resilient to variation in operating conditions. Both refrigerant charge and the pressure drop are less than or equal to the baseline under the corresponding modes.

As a result of optimization using Formulation (2), the optimal design by minimizing refrigerant charge yields a charge reduction of 19.2% under AC mode and the charge reduction by 21.6% under HP mode. Meanwhile its capacity is slightly higher than the baseline under the corresponding operating modes.

Table 4: Summary of Optimization Results

Case	**Baseline**		**Single-obj. Optimal (Maximize Q)**		**Bi-objective Optimal (Maximize Q)**		**Bi-objective Optimal (Minimize Charge)**	
Mode	AC	HP	AC	HP	AC	HP	AC	HP
Capacity [W]	5294	5845	5421 (2.4%↑)	5177 (11.4%↓)	5418 (2.3%↑)	6021 (3.0%↑)	5305 (0.2%↑)	5918 (1.2%↓)
Ref. DP [kPa]	11.9	7.3	11.7 (1.7%↓)	7.3 (-)	11.9 (-)	6.5 (11.0%↓)	11.7 (1.6%↓)	6.6 (9.6%↓)
Sensible Heat Ratio	79.9%	100%	80.6%	100%	79.8%	100%	79.5%	100%
Outlet Saturation ΔT [K] (+ superheat, - subcooling)	+8.4	-9.48	+9.4	-8.5	+8.7	-10.13	+8.85	-10.02
Refrigerant Charge [g]	182.5	877.8	168.9 (7.5%↓)	828.5 (5.6%↓)	161.0 (11.8%↓)	877.8 (-)	147.5 (19.2%↓)	688.3 (21.6%↓)

Table 5 presents the circuitry of the baseline, the single objective optimal design and the bi-objective optimal designs from problem Formulation (1) and Formulation (2). In the circuitry plots, a solid line represents a U-bend on the near end of the heat exchanger, while a dotted line represents a U-bend on the far end. The red tubes are the inlets, while the blue ones are outlets. Merging tubes and splitting tubes are represented by yellow and black circles, respectively. In terms of manufacturability, the baseline has 2 long U-bends spanning over 3 tube rows, while all U-bends from the optimal designs are shorter than 3 tube rows.

Table 5: Circuitry of Baseline and Optimal Designs

Case	Baseline		Single-obj. Optimal (Maximize Q)		Bi-objective Optimal (Maximize Q)		Bi-objective Optimal (Minimize Charge)	
Mode	AC	HP	AC	HP	AC	HP	AC	HP
Circuitry	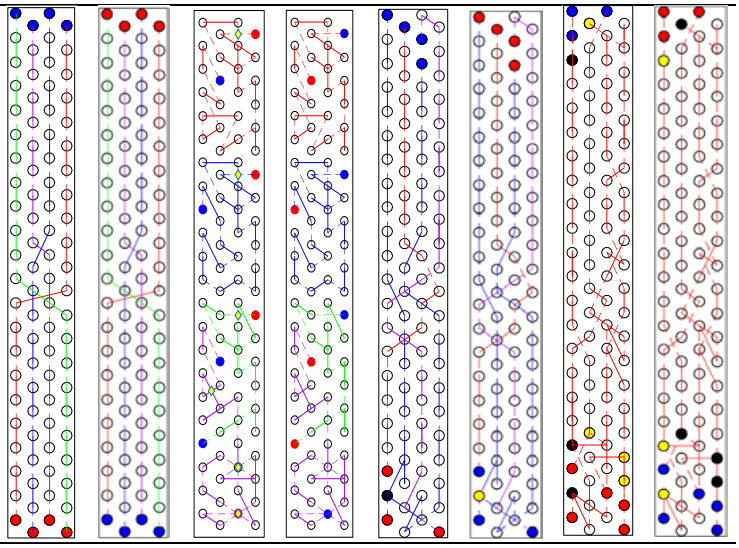							
U-bends (Length ≤ 2 tube rows)	82	82	84	84	85	85	87	87
U-bends (Length > 2 tube rows)	2	2	0	0	0	0	0	0

5.3. System level result

In order to test the system performance of the optimal designs and the baseline, a component-based vapor compression simulation tool [30] is used to simulate a realistic reversible heat pump cycle which is experimentally validated [29] using the baseline HX as the indoor coil. Fig. 7(a) and Fig. 7(b) show the schematic of the reversible heat pump system under cooling mode and heating mode, respectively. The information of other components (outdoor HX, compressor, expansion device) is detailed in the original paper [29]. The test condition is the ANSI/AHRI Standard 210/240 A cooling and heating conditions [31].

In Fig. 7(a) and Fig. 7(b), the air flow maldistribution profile simulated using an OpenFOAM® based CFD model ([32]) can be observed at the frontal face of A-type indoor unit. The air velocity at the apex is largest and the air velocity decreases from top to bottom of the coil.

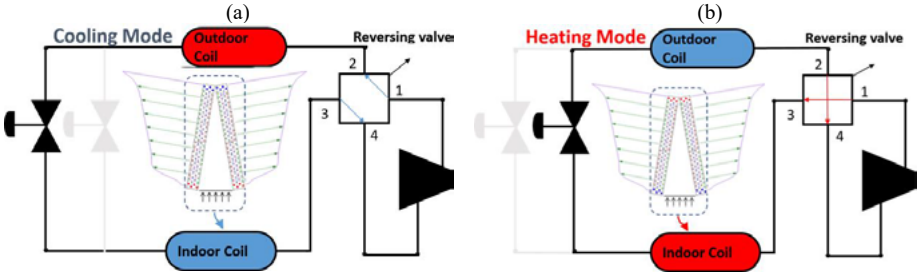

Fig. 7. Schematic of Reversible Heat Pump System: (a) Cooling (i.e. AC) Mode Operation; (b) Heating (i.e. HP) Mode Operation

Fig. 8 shows the system performance of the reversible heat pump system using the baseline or the optimal circuitry designs as indoor coil. Under cooling mode (Fig. 8(a)), the optimal design by maximizing capacity gains COP improvement from 3.54 to 3.63 by 2.5%, but the optimal design by minimizing refrigerant charge

only leads to COP improvement from 3.54 to 3.55 by 0.3%. Meanwhile, under heating mode (Fig. 8(b)), the optimal design by maximizing capacity gains COP improvement from 4.61 to 4.74 by 2.8%, but the optimal design by minimizing refrigerant charge only leads to COP improvement from 4.61 to 4.65 by 0.8%.

From the P-h diagrams, when the optimal design by maximizing capacity (red line in Fig. 8) operates as an evaporator in AC mode, it induces higher evaporating temperature. When it operates as a condenser in HP mode, it induces lower condensing temperature. Thus, the system efficiency is improved.

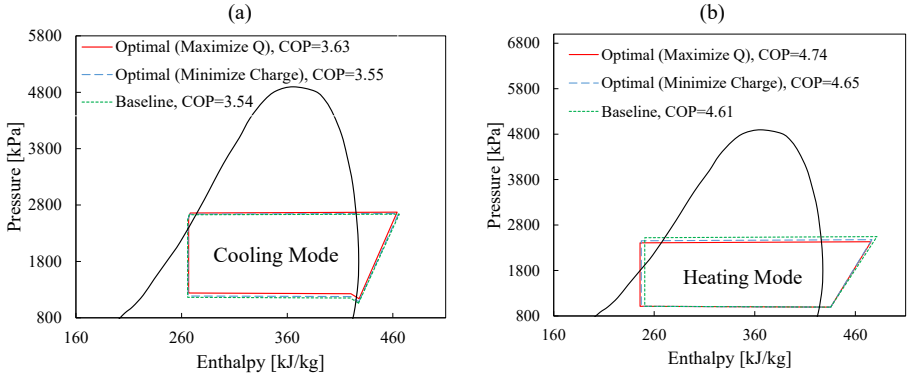

Fig. 8. R410A P-h diagram using Different Circuitry Designs in Indoor Unit: (a) Cooling mode; (b) Heating mode

6. Conclusion

This paper presents a newly developed tube-fin heat exchanger circuitry optimization algorithm. A new chromosome representation and eight GA operators are developed to extend the capability of Integer Permutation based Genetic Algorithm. In order to obtain optimal circuitries with improved performance under both air conditioning and heat pump modes for reversible heat pump system, two multi-objective problem formulations are explored. Case studies using an A-type indoor unit from a reversible heat pump system shows that the optimal design using the formulation with the objective to maximize heat exchanger capacity leads to 2.3% (AC mode) and 3.0% (HP mode) capacity improvement. In addition, it yields COP improvement by 2.5% (AC mode) and 2.8% (HP mode). Considering the single-objective optimal design obtained under solely AC mode induces 11.4% capacity degradation if it is used in HP mode, the effective capacity improvement of the bi-objective optimal is 14.4%. The optimal design obtained using the formulation with the objective to minimize refrigerant charge effectively reduce heat exchanger refrigerant charge by 19.2% (AC mode) and 21.6% (HP mode), meanwhile maintaining the heat exchanger capacity and COP to be the similar amount as the baseline. Use of the proposed circuitry optimization approach in early design stages can help assure a certain minimum robust performance of heat exchangers in heat pumps during both cooling and heating mode usage as well as assist in redesign of existing heat exchangers for new lower-GWP refrigerants.

Acknowledgements

This work was supported by the Modeling and Optimization Consortium of the Center for Environmental Energy Engineering at the University of Maryland.

References

[1] L. Huang, V. Aute, and R. Radermacher. A Survey of Optimization Formulations and Techniques for the Design of Heat Exchangers Using Lower Gwp Refrigerants. ASHRAE Winter Conference. (2015)

[2] M. Chwalowski, D. Didion, and P. Domanski. Verification of Evaporator Computer Models and Analysis of Performance of an Evaporator Coil. ASHRAE Transactions 95 (1989): 1229-36.

[3] C. C. Wang, et al. Effect of Circuit Arrangement on the Performance of Air-Cooled Condensers. International Journal of Refrigeration 22.4 (1999): 275-82.

[4] G. Bigot, L. Palandre, and D. Clodic. Optimized Design of Heat Exchangers for" Reversible" Heat Pump Using R-407C. International Refrigeration and Air Conditioning Conference. Purdue, USA. (2000).

[5] S. Liang, T. Wong, and G. Nathan. Numerical and Experimental Studies of Refrigerant Circuitry of Evaporator Coils. International Journal of Refrigeration 24.8 (2001): 823-33.
[6] W. Ding, et al. A General Simulation Model for Performance Prediction of Plate Fin-and-Tube Heat Exchanger with Complex Circuit Configuration. Applied Thermal Engineering 31.16 (2011): 3106-16.
[7] H.Y. Ye, and K.S. Lee. Refrigerant Circuitry Design of Fin-and-Tube Condenser Based on Entropy Generation Minimization. International Journal of Refrigeration 35.5 (2012): 1430-38.
[8] C. M. Joppolo, L. Molinaroli, and A. Pasini. Numerical Analysis of the Influence of Circuit Arrangement on a Fin-and-Tube Condenser Performance. Case Studies in Thermal Engineering 6 (2015): 136-46.
[9] D. A. Yashar, et al. A Dual-Mode Evolutionary Algorithm for Designing Optimized Refrigerant Circuitries for Finned-Tube Heat Exchangers. HVAC&R Research 18.5 (2012): 834-44.
[10] P. A. Domanski, and D. Yashar. Application of an Evolution Program for Refrigerant Circuitry Optimization, Proceedings of ACRE Conference, New Delhi, India (2007).
[11] P. A. Domanski, and D. Yashar. Optimization of Finned-Tube Condensers Using an Intelligent System. International Journal of Refrigeration 30.3 (2007a): 482-88.
[12] H. Cho, and P. A. Domanski. Optimized Air-to-Refrigerant Heat Exchanger with Low-GWP Refrigerants. 12th IIR Gustav Lorentzen Natural Working Fluids Conference, UK, Edinburgh (2016).
[13] D. A. Yashar, S. Lee, and P. A. Domanski. Rooftop Air-Conditioning Unit Performance Improvement Using Refrigerant Circuitry Optimization. Applied Thermal Engineering 83 (2015): 81-87.
[14] Z. Wu, et al. Application of a Genetic Algorithm to Optimize the Refrigerant Circuit of Fin-and-Tube Heat Exchangers for Maximum Heat Transfer or Shortest Tube. International Journal of Thermal Sciences 47.8 (2008b): 985-97.
[15] Z. Wu, et al. Knowledge-Based Evolution Method for Optimizing Refrigerant Circuitry of Fin-and-Tube Heat Exchangers. HVAC&R Research 14.3 (2008a): 435-52.
[16] N. Ploskas, et al. Optimization of Circuitry Arrangements for Heat Exchangers Using Derivative-Free Optimization. Chemical Engineering Research and Design 131 (2018): 16-28.
[17] Z. Li, J. Ling, and V. Aute. Tube-fin Heat Exchanger Circuitry Optimization Using Integer Permutation Based Genetic Algorithm. International Journal of Refrigeration. 103 (2019): 135-144.
[18] K. Deb. Optimization for Engineering Design: Algorithms and Examples. PHI Learning Pvt. Ltd., 2012.
[19] Z. Li, and V. Aute. Optimization of Heat Exchanger Flow Paths Using a Novel Integer Permutation Based Genetic Algorithm. EngOpt 2018 Proceedings of the 6th International Conference on Engineering Optimization, Lisboa, Portugal (2018).
[20] ASHRAE. Methods of Testing for Rating Seasonal Efficiency of Unitary Air Conditioners and Heat Pumps. ANSI/ASHRAE Standard (2010): Atlanta, GA, USA.
[21] F. Dittus, and L. Boelter. Heat Transfer in Automobile Radiators of the Tubular Type. International Communications in Heat and Mass Transfer 12.1 (1985): 3-22.
[22] H. Blasius. Grenzschichten in Flüssigkeiten Mit Kleiner Reibung. Druck von BG Teubner, 1907.
[23] D. Jung, et al. A Study of Flow Boiling Heat Transfer with Refrigerant Mixtures. International Journal of Heat and Mass Transfer 32.9 (1989): 1751-64.
[24] D. Jung, and R. Radermacher. Prediction of Pressure Drop During Horizontal Annular Flow Boiling of Pure and Mixed Refrigerants. International Journal of Heat and Mass Transfer 32.12 (1989): 2435-46.
[25] A. Cavallini, et al. Condensation in Horizontal Smooth Tubes: A New Heat Transfer Model for Heat Exchanger Design. Heat Transfer Engineering 27.8 (2006): 31-38.
[26] R. Lockhart, and R. Martinelli. Proposed Correlation of Data for Isothermal Two-Phase, Two-Component Flow in Pipes. Chem. Eng. Prog 45.1 (1949): 39-48.
[27] C. C. Wang, et al. Heat Transfer and Friction Correlation for Compact Louvered Fin-and-Tube Heat Exchangers. International journal of heat and mass transfer 42.11 (1999): 1945-56.
[28] H. Jiang, V. Aute, and R. Radermacher. Coildesigner: A General-Purpose Simulation and Design Tool for Air-to-Refrigerant Heat Exchangers. International Journal of Refrigeration 29.4 (2006): 601-10.
[29] A. Alabdulkarem, et al. Testing, Simulation and Soft-Optimization of R410a Low-GWP

Alternatives in Heat Pump System. International Journal of Refrigeration 60 (2015): 106-17.
[30] J. Winkler, V. Aute, and R. Radermacher. Component-Based Vapor Compression Simulation Tool with Integrated Multi-Objective Optimization Routines. International Refrigeration and Air Conditioning Conference. Purdue Univ. (2006).
[31] AHRI. Standard 210/240-2008. Performance Rating of Unitary Air Conditioning and Air-Source Heat Pump Equipment. AHRI (2008)
[32] M. S. Lee, et al. A CFD Assisted Segmented Control Volume Based Heat Exchanger Model for Simulation of Air-to-Refrigerant Heat Exchanger with Air Flow Mal-Distribution. Applied Thermal Engineering 131 (2018): 230-43.